Microfluidic High-Resolution Free-Flow Isoelectric Focusing

Dietrich Kohlheyer,* Jan C. T. Eijkel, Stefan Schlautmann, Albert van den Berg, and Richard B. M. Schasfoort

MESA+ Institute for Nanotechnology, University of Twente, P.O. Box 217, 7500AE Enschede, The Netherlands

A microfluidic free-flow isoelectric focusing glass chip for separation of proteins is described. Free-flow isoelectric focusing is demonstrated with a set of fluorescent standards covering a wide range of isoelectric points from pH 3 to 10 as well as the protein HSA. With respect to an earlier developed device, an improved microfluidic FFE chip was developed. The improvements included the usage of multiple sheath flows and the introduction of preseparated ampholytes. Preseparated ampholytes are commonly used in large-scale conventional free-flow isoelectric focusing instruments but have not been used in micromachined devices yet. Furthermore, the channel depth was further decreased. These adaptations led to a higher separation resolution and peak capacity, which were not achieved with previously published free-flow isoelectric focusing chips. An almost linear pH gradient ranging from pH 2.5 to 11.5 between 1.2 and 2 mm wide was generated. Seven isoelectric focusing markers were successfully and clearly separated within a residence time of 2.5 s and an electrical field of 20 V mm^{-1}. Experiments with pI markers proved that the device is fully capable of separating analytes with a minimum difference in isoelectric point of $\Delta(pI) = 0.4$. Furthermore, the results indicate that even a better resolution can be achieved. The theoretical minimum difference in isoelectric point is $\Delta(pI) = 0.23$ resulting in a peak capacity of 29 peaks within 1.8 mm. This is an 8-fold increase in peak capacity to previously published results. The focusing of pI markers led to an increase in concentration by factor 20 and higher. Further improvement in terms of resolution seems possible, for which we envisage that the influence of electroosmotic flow has to be further reduced. The performance of the microfluidic free-flow isoelectric focusing device will enable new applications, as this device might be used in clinical analysis where often low sample volumes are available and fast separation times are essential.

In proteomics analysis, protein separation is often achieved by two-dimensional gel electrophoresis (2D GE). To decrease the high sample complexity of proteins present in blood sera or cell extracts prior to a 2D GE separation, free-flow electrophoresis (FFE) has found its place as a preanalytical prefractioning tool.[1−3] Free-flow electrophoresis allows the fractioning of particles, cells, organelles, and macromolecules based on their electrophoretic mobility transverse to a hydrodynamic carrier flow.[4]

One mode of FFE is free-flow isoelectric focusing (FFIEF), in which a pH gradient is established perpendicular to the carrier flow. This pH gradient is achieved and buffered by adding ampholytes to the solution. These ampholytes have specific isoelectric points and rearrange by migration when an electrical field is applied.[5] Proteins migrate due to the applied external field along the pH gradient and eventually get focused where the local pH value is equal to their pI value, at which point their net charge is zero.[6,7] The main disadvantage of applying FFE and FFIEF is the requirement for high sample volumes, typically ranging from a few milliliters to a few tens of milliliters. Especially in clinical analysis with often low amounts of patients sample available, miniaturization of FFE is therefore promising.[8,9] Miniaturized microfluidic FFE systems allow easier control of laminar flow, as well as the possibility to apply higher separation voltages without Joule heating problems.[10] These advantages were already recognized by Raymond et al. in 1994 who presented the first microfluidic FFE device (μ-FFE).[11] In the past years, several μ-FFE systems, including microfluidic versions of FFIEF, were developed and the separation efficiency was further improved.[12−19] The

(1) Weber, G.; Islinger, M.; Christoph, P. W.; Völkl, E. A. *Electrophoresis* **2004**, *25*, 1735−1747.
(2) Obermaier, C.; Jankowski, V.; Schmutzler, C.; Bauer, J.; Wildgruber, R.; Infanger, M.; Köhrle, J.; Krause, E.; Weber, G.; Grimm, D. *Electrophoresis* **2005**, *26*, 2109−2116.
(3) Poggel, M.; Melin, T. *Electrophoresis* **2001**, *22*, 1008−1015.
(4) Krivánková, L.; Bocek, P. *Electrophoresis* **1998**, *19*, 1064−1074.
(5) Horka, M.; Willimannb, T.; Blumb, M.; Nordingb, P.; Friedlc, Z.; Slais, K. *J. Chromatogr., A* **2001**, *916*, 65−71.
(6) Soulet, N.; Balmann, H. R.-d.; Sanchez, V. *Electrophoresis* **1998**, *19*, 1294−1299.
(7) Weber, G.; Bo, P. *Electrophoresis* **1998**, *19*, 1649−1653.
(8) Janasek, D.; Franzke, J.; Manz, A. *Nature* **2006**, *442*, 374−380.
(9) Dittrich, P. S.; Tachikawa, K.; Manz, A. *Anal. Chem.* **2006**, *78*, 3887−3908.
(10) Lion, N.; Rohner, T. C.; Dayon, L.; Arnaud, I. L.; Damoc, E.; Youhnovski, N.; Wu, Z.-Y.; Roussel, C.; Josserand, J.; Jensen, H.; Rossier, J. S.; Przybylski, M.; Girault, H. H. *Electrophoresis* **2003**, *24*, 3533−3562.
(11) Raymond, D. E.; Manz, A.; Widmer, H. M. *Anal. Chem.* **1994**, *66*, 2858−2865.
(12) Raymond, D. E.; Manz, A.; Widmer, H. M. *Anal. Chem.* **1996**, *68*, 2515−2522.
(13) Chartogne, A.; Tjaden, U. R.; Greef, J. V. d. *Rapid Commun. Mass Spectrom.* **2000**, *14*, 1269−1274.
(14) Kobayashi, H.; Shimamura, K.; Akaida, T.; Sakano, K.; Tajima, N.; Funazaki, J.; Suzuki, H.; Shinohara, E. *J. Chromatogr., A* **2003**, *990*, 169.
(15) Xu, Y.; Zhang, C. X.; Janasek, D.; Manz, A. *Lab Chip* **2003**, *3*, 224−227.
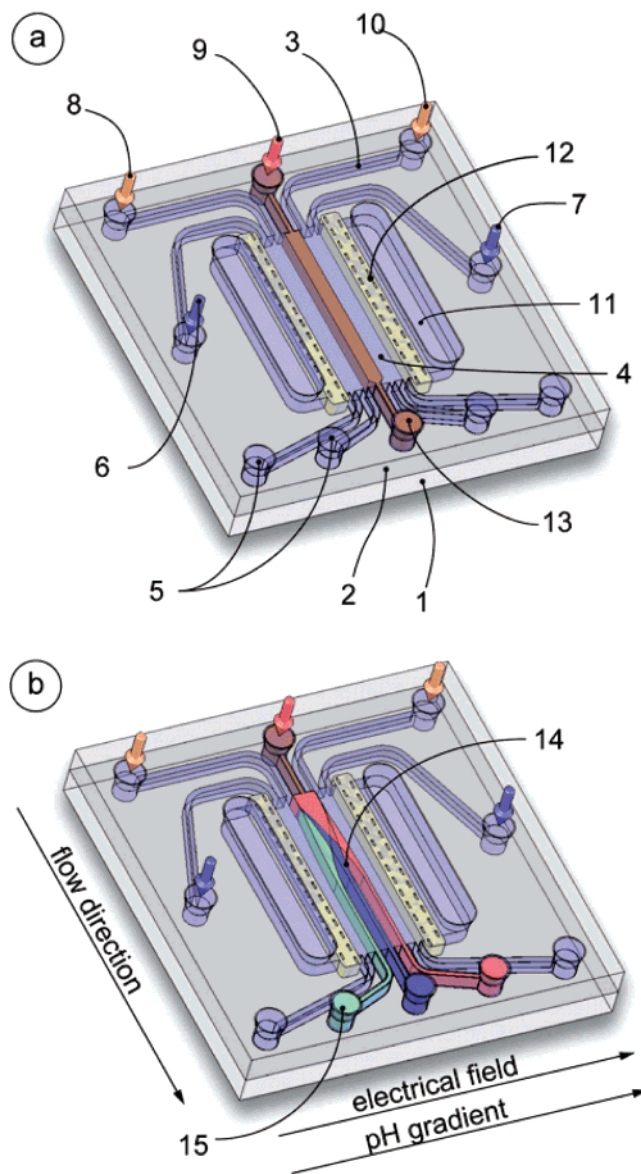(16) Zhang, C.-X.; Manz, A. *Anal. Chem.* **2003**, *75*, 5759−5766.

* Corresponding author. E-mail: d.kohlheyer@utwente.nl. Phone: +31 53 489 1051.

particular interest in μ-FFE systems is growing rapidly, indicated by the relatively high number of publications in 2006.[20−27] Although the system performance of microfluidic FFE and FFIEF was steadily improved, resulting in faster separation, higher voltage efficiency, and increased resolution, the published results so far are not sufficient compared to large-scale conventional FFE systems. Besides the presentation of a new FFIEF chip, one of the aims of this paper was to study more intensively the performance-limiting factors in μ-FFIEF systems and how to further increase the separation performance.

Here we report on an improved microfluidic FFIEF chip, developed by learning from the large-scale FFE instruments currently available and miniaturizing certain aspects, namely, multiple sheath flows and preseparated ampholytes.[28] This microfluidic chip device was characterized with a set of fluorescent IEF standards covering isoelectric points ranging from pH 3 to 11. In terms of separation peak capacity and resolution, the results surpass all thus far published devices.

PRINCIPLE

The FFIEF chip presented here is a further development of an earlier published version, and for some details the reader is referred to this paper.[27] As illustrated in Figure 1, the μ-FFIEF chip consists of a bottom glass plate (1), which is left unprocessed, and a top glass plate (2), which incorporates a network of microfluidic channels (3) and the separation chamber (4). The bottom glass plate is bonded to the upper plate in order to seal the microfluidic network. Inlets and outlets (5) through the top plate provide access for fluidic connections. The separation chamber is connected to five inlet channels used to fill the chamber with different flow streams. Each stream serves a different purpose. The two outer inlet channels (6, 7) are used to infuse the separation chamber sides with a sheath flow of low pH and of high pH, respectively, to confine the limits of the applied pH gradient. The three inner inlet channels (8−10) are used to fill the chamber with the required ampholytes to buffer the pH gradient. A detailed explanation is found along with Figure 2. The center inlet channel (9) is also used to bring in the sample mixture. To couple the electrical field in, the chip has two parallel open electrode compartments (11) filled with an electrolyte solution into which two external platinum wires are placed. Two ion-permeable hydrogel membranes (12) at the sides of the separation

(17) Lu, H.; Gaudet, S.; Schmidt, M. A.; Jensen, K. F. *Anal. Chem.* **2004**, *76*, 5705−5712.
(18) Albrecht, J.; Gaudet, S.; Jensen, K. F. *μ-TAS 2005*, Boston, MA, 2005; pp 1537−1539.
(19) Fonslow, B. R.; Bowser, M. T. *Anal. Chem.* **2005**, *77*, 5706−5710.
(20) Albrecht, J.; Jensen, K. F. *μ-TAS 2006*, Tokyo, Japan, 2006; pp 921−923.
(21) Albrecht, J. W.; Jensen, K. F. *Electrophoresis* **2006**, *27*, 4960−4969.
(22) Fonslow, B. R.; Barocas, V. H.; Bowser, M. T. *Anal. Chem.* **2006**, *78*, 5369−5374.
(23) Fonslow, B. R.; Bowser, M. T. *Anal. Chem.* **2006**, *78*, 8236−8244.
(24) Janasek, D.; Schilling, M.; Franzke, J.; Manz, A. *Anal. Chem.* **2006**, *78*, 3815−3819.
(25) Janasek, D.; Schilling, M.; Manz, A.; Franzke, J. *Lab Chip* **2006**, *6*, 710−713.
(26) Jesus, D. P. d.; Blanes, L.; Lago, C. L. d. *Electrophoresis* **2006**, *27*, 4935−4942.
(27) Kohlheyer, D.; Besselink, G. A. J.; Schlautmann, S.; Schasfoort, R. B. M. *Lab Chip* **2006**, *6*, 374−380.
(28) Weber, P. J. A.; Weber, G.; Eckerskom, C. In *Purifying Proteins for Proteomics: A Laboratory Manual*; Simpson, R. J., Ed.; Cold Spring Harbor Laboratory Press: New York, 2003.

Figure 1. μ-FFIEF chip layout and working principle: (a) no voltage applied; no separation (b) voltage applied, IEF of three components. (1, bottom chip plate; 2, top chip plate; 3, microfluidic channel; 4, separation chamber; 5, outlets; 6, low-pH sheath flow inlet; 7, high-pH sheath flow inlet; 8, ampholytes 1 inlet; 9, ampholytes 2 + sample inlet; 10, ampholytes 3 inlet; 11, electrode compartment; 12, conductive membrane; 13, not separated sample; 14, focused sample; and 15, collected sample).

chamber (4) form an electrically conducting, but a fluid leakage minimized bridge between the electrode compartments and the separation region. In this way, a stable electrical field can be applied and gas formation at the electrodes due to electrolysis will not disturb the separation. Figure 1a illustrates the device when no voltage is applied and the sample mixture exits the device unseparated (13). When an electrical field is applied across the separation region (Figure 1b), the continuously flowing ampholytes rearrange by migration to form the pH gradient and the sample components (14) migrate toward and focus at their isoelectric points. The fractions can be collected separately (15). The number of chip outlets was limited to five for practical reasons and does not correspond to the number of separated analytes.
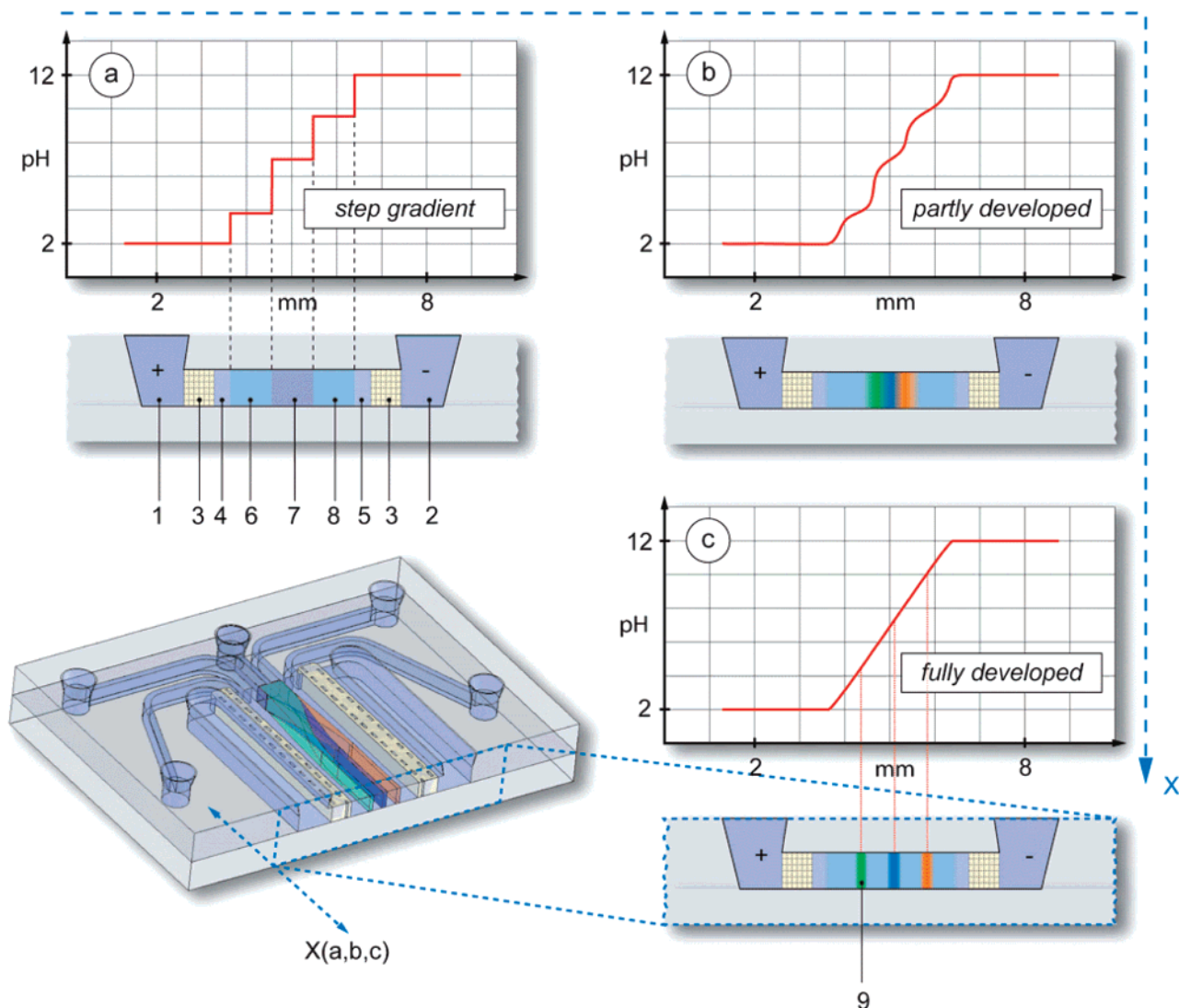
Figure 2. pH gradient formation using preseparated ampholytes: (a–c) show a cross section of the separation chamber at different positions *x* and the corresponding pH gradient. With the increasing residence time, the pH gradient is further developing. (1, anodic electrolyte; 2, cathodic electrolyte; 3, membrane; 4, acidic sheath flow; 5, basic sheath flow; 6, prolyte1; 7, prolyte2 + sample; 8, prolyte3; 9, fully focused sample component).

Conventional large-scale FFE systems, such as that introduced to the market by BD-Biosciences, use several inlets to fill the separation chamber with preseparated ampholytes. The usage of these preseparated ampholytes results in a lower electrical current and faster separation times, since the amphoteric substances need less time to reach their respective pI values. BD provides their standard ampholytes covering a pH range from 2.5 to 11.5. Here we refer to these preseparated ampholyte reagents as prolytes1, prolytes2, and prolytes3.

In Figure 2, the application of preseparated ampholytes is illustrated in more detail. The illustration shows three cross sections (Figure 2a–c) of the chip separation chamber. Each cross section corresponds to a different *x*-coordinate (x_a, x_b, x_c) along the chamber. Since it is a continuously flowing system, each position directly corresponds to a specific residence time depending on the flow velocity. To clarify the formation of the pH gradient, diagrams of the expected pH gradient are shown. Observing the cross section directly at the separation chamber entrance (Figure 2a), one can see that the chamber is infused

with five adjacent fluid streams. (With no electrical field applied, these streams would only mix by diffusion.) The positive anode (1) is placed in an acidic solution of pH 2 while the cathode (2) is inserted into a basic solution of pH 12. The separation chamber is shielded by two ion-permeable membranes (3). Next to the membranes, two sheath flow streams of pH 2 (4) and pH 12 (5) confine the outer limits of the applied pH gradient. Depending on the ampholytes reagents used, the electrolyte and sheath flow pH values might differ. However, here only a wide pH range gradient (pH 2.5–11.5) was used. The inner three streams contain the ampholytes prolytes1 (6), prolytes2 (7), and prolytes3 (8). Furthermore, the center stream (7) also contains the sample mixture. In this manner, a stepped pH gradient is generated. With increasing residence time (Figure 1b) of the ampholytes in the electrical field, a continuous pH gradient starts to form due to migration of the ampholytes toward their pI. Past a certain position, which depends on the flow rate and applied voltage, a linear pH gradient (Figure 2c) has fully developed and all sample components focus (9) at their isoelectric point.

EXPERIMENTAL SECTION

Materials and Reagents. Fluorescent IEF standards and proteins were purchased from Sigma-Aldrich-Fluka. Proteins were labeled by Active Motif Chromeon using the CE-540 fluorescent dye. Ampholyte solutions prolytes1, 2, and 3 were obtained from BD Diagnostics. All other chemicals were obtained from Sigma-Aldrich-Fluka. All solutions were degassed in vacuum for 10 min to minimize air bubbles during flow operations.

Chip Fabrication. Each chip consists of two thermally bonded Borofloat 33 glass plates (Schott Jenaer Glass); the top plate contains the channels, separation chamber, fluidic inlets and outlets, and electrode openings, while the bottom plate is unprocessed. Hydrofluoric acid was used to etch the channels and separation chamber while a chromium–gold layer protected the regions not to be etched. The etch depth was 10 μm. A powder blasting step was performed with Al_2O_3 particles to create the inlet and outlet holes, as well as the electrode openings. The processed glass wafer was thermally bonded to another borofloat glass wafer. The bonded wafers were finally diced into several microfluidic chips. A silanization step with trimethoxysilylpropylmethacrylate was performed to achieve a chemical bond between the acrylamide membranes and the glass surface to increase the stability. An acrylamide solution, including a cross-linker and photoinitiator, was used to fill the chip and was exposed through a slit mask using a UV light source. The photopolymerized acrylamide regions form the desired membranes. Finally the chips were filled with a solution of 1% poly(vinyl alcohol) (PVA) in DI water and incubated overnight, to coat the channel surface to minimize electroosmotic flow (EOF) as well as protein absorption.

Experimental Setup and Methods. The fabricated chips were placed in an in-house fabricated holder. Syringe pumps (CMA/102, Microdialysis) were used to control the flow rates. The 1-mL glass syringes (Microdialysis) were filled with the required solutions and connected via glass capillaries (Aurora) and Nanoport connectors (Upchurch Scientific) with the chip holder. Two integrated platinum electrodes were mounted inside the electrode compartments and connected to a power supply (Labsmith). Power supply and syringe pumps were controlled in real time with a personal computer and the software LabView (National Instruments). Both electrolyte reservoirs were connected via polymer tubes to a peristaltic pump (Ismatec) to ensure a continuous refreshment of the solutions. The holder was placed on a fluorescence microscope (Olympus IX51) equipped with mercury burner and fluorescent filter set (XF02-2, Omega Optical). Images were captured with the digital color camera ColorViewII (Soft Imaging Systems) and recorded with the software package AnalySIS 5 (Soft Imaging Systems).

For most of the FFIEF experiments the following conditions were used: The anodic electrolyte reservoir was filled with 20 mM H_2SO_4 and the cathodic electrolyte reservoir with 20 mM NaOH. All inner fluid streams (Figure 2a, streams 4–8) contained 0.1% hydroxypropylmethylcellulose (HPMC) to reduce EOF and 0.1% Tween-20 to increase solubility of sample components, but more importantly to reduce the solution surface tension allowing air bubbles trapped in the channels to be removed more quickly. The acidic sheath flow (stream 4, stream numbers correspond with the numbers given in Figure 2a and Figure 4a) contained 20 mM H_2SO_4 while the alkaline sheath (stream 5) contained 20 mM
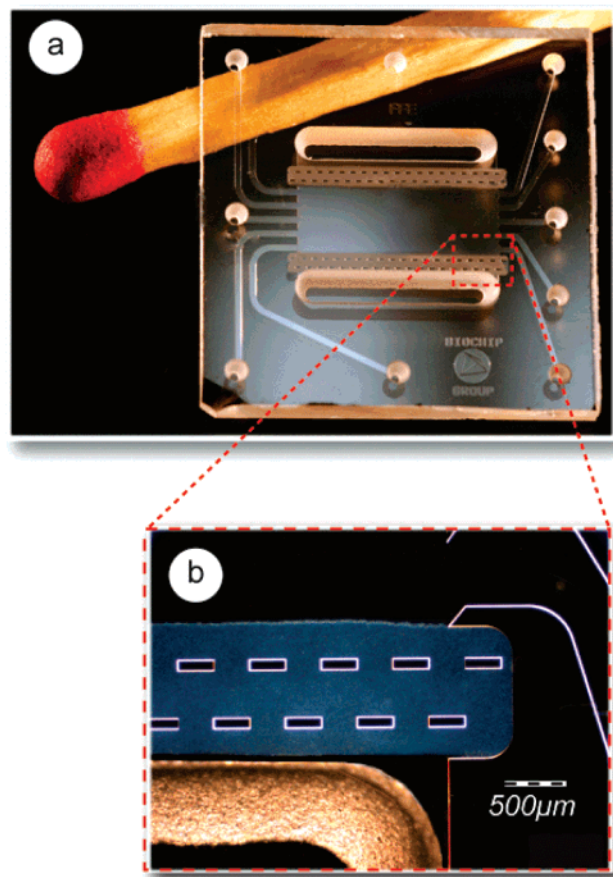


Figure 3. Photographs of a fabricated μ-FFIEF chip. (a) The chip size is 20 mm × 20 mm with a thickness of 2.2 mm. The separation chamber has a volume of 0.35 μL ($h \times w \times l$: 10 μm × 3.5 mm × 10 mm). (b) Closeup of one of the membranes. The membranes are supported by glass structures to increase mechanical stability.

NaOH. The ampholyte streams (streams 6–8) contained 20% of polytes1, prolytes2, and prolytes3, respectively. The sample stream (stream 7) contained additionally a mixture of fluorescent IEF markers or proteins. All experiments were conducted at a flow velocity of 2 mm s^{-1}.

RESULTS AND DISCUSSION

Fabricated Chips. A fabricated chip can be seen in Figure 3a. The glass chip is 20 mm × 20 mm in size and has a thickness of 2.2 mm. The etched channel depth is 10 μm. The five inlet channels and outlet channels are 300 μm in width. The size of the separation chamber is 10 mm in length and 3.5 mm in width, resulting in a volume of 0.35 μL. However, in practice, only 30–60% of the total width is used for separation. The practical width of the separation region can easily be varied by adjusting the width of the outer sheath flows (streams 4 and 5 in Figure 2). While maintaining the total flow rate, a wider low-pH and high-pH sheath flow stream (confining the limits of the used pH gradient) results in less space for the actual pH gradient. Width adjustments are performed by controlling the flow rates of the appropriate syringe pumps. As shown in the dark-field microscopy image (Figure 3b), the width of the membranes between electrode opening and separation chamber is ~1 mm. To enhance the mechanical strength of the membranes and to withstand the pressure-driven fluid inside the chamber, several glass pillars were included.
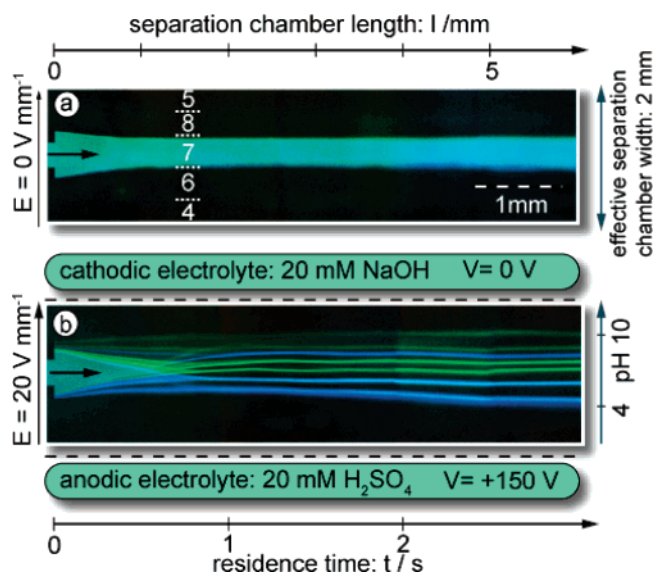
Figure 4. Free-flow isoelectric focusing of 7 fluorescent IEF markers: (a) Photograph shows the device, when no voltage was applied. The white numbers directly correspond to the stream numbers given in Figure 2. (b) When 150 V ($I = 50\ \mu A$) was applied, the markers (pI 4, 5.1, 6.2, 7.2, 8.1, 9, and 10.3) fully separated within less than 2 s. The sample flow rate was 0.4 μL min^{-1} ($v = 2$ mm s^{-1}) The apparent kinks in the fluorescent tracer paths are caused by merging multiple photographs.

FFIEF of Fluorescent Low MW IEF Markers. pH Gradient Quality. The use of low molecular weight fluorescent isoelectric focusing markers has proven to be an accurate method to characterize IEF systems. In contrast to protein standards, they show a lower tendency to precipitate at their pI due to a better solubility.[5] To cover a broad range of pH values, the following fluorescent IEF markers were selected: pI 3, 4, 5.1, 5.5, 6.2, 7.2, 7.6, 8.1, 9, and 10.3.

Figure 4 shows two photographs taken during FFIEF experimental work to clarify the working principle. The images show a 6-mm-long part of the separation chamber with the flow being from left to right. The total flow velocity inside the chamber was set to 2 mm s^{-1}. As long as no voltage was applied, the adjacent streams did not mix except by diffusion (Figure 4a). When an electrical field of 20 V mm^{-1} was applied (voltage $V = 150$ V, current $I = 50\ \mu A$), separation and focusing of all IEF standards was observed. After a residence time of less than 2 s, all seven IEF markers were separated and after 3 s the focusing was completed (Figure 4b).

The applied ampholyte system uses amphoteric substances with equal differences in isoelectric points over the whole pH range, resulting in a linear pH gradient. Assuming all IEF markers focus exactly at their isoelectric points, one could derive the pH gradient that is actually achieved. Therefore, a fluorescence intensity plot was generated (Figure 5b) from a FFIEF experiment using seven IEF markers (Figure 5a). Based on the peak positions, the experimentally interpolated pH gradient was derived as shown in Figure 5c. It can be seen that the pH gradient was fully developed and furthermore that the gradient linearity was close to ideal.

Peak Width. According to Giddings, a useful parameter system to express the quality of an equilibrium gradient separation system, such as isoelectric focusing, includes the standard deviation of the peak width (σ), minimum pI value (Δ(pI)$_{min}$), and peak capacity (n).[29] Assuming a Gaussian concentration distribution, the standard deviation for a peak generated in IEF is given by

$$\sigma = \sqrt{D/pE} \qquad (1)$$

where D is the diffusion coefficient, E the electrical field strength, and

$$p = -\frac{d\mu}{d(pH)}\frac{d(pH)}{dx} \qquad (2)$$

Here $d(pH)/dx$ is the pH gradient slope and $d\mu/d(pH)$ the mobility slope of the analyte.[30] For the separation results shown in Figure 5, we derived the peak standard deviations. The results are given in Table 1 and result in an average $\sigma = 19\ \mu$m.

Of the variables in eq 1, the diffusion coefficient and mobility slope are intrinsic properties of the analytes, so that only the electrical field and the pH gradient can be varied experimentally to reduce the peak width. Obviously, a shallower pH gradient would lead to higher resolving power but within a more limited pH range. The present device was designed for a constant wide range pH gradient (pH 2.5–11.5). Therefore, only the electrical field was varied during experiments. Equation 1 predicts that a high electrical field decreases the peak width. To investigate the influence of the electrical field, the average standard deviation σ_{av} was determined for various electrical field settings and the results are shown in Figure 6.

As shown in Figure 6, for electrical field strengths below 10 V mm^{-1}, we observed an approximately linear decrease of σ. We concluded from the current/voltage curves, to be shown in Figure 7 and discussed there, that this improvement in peak width is directly related to the pH gradient formation and that a minimum electrical field of 15 V mm^{-1} is required to reach a fully developed and steady-state pH gradient at the flow velocity of $v = 2$ mm s^{-1}. In contrast to the theory given by eq 1, an increasing electrical field did not reduce the peak width any further, but between 10 and 40 V mm^{-1}, the average standard deviation reached a constant value of ~18 μm. Furthermore, fields above $E = 50$ V mm^{-1} caused increasing band broadening and eventually destabilization of the separation (data not shown here; see also Figure 8). Possible reasons that might explain the lack of a further decrease in peak width above $E = 10$ V mm^{-1} can be Joule heating and electroosmotic flow. Both parameters are well-known from free-flow electrophoresis leading to band broadening in the form of a crescent-shaped deformation of the sample.[31] We will first consider the influence of Joule heating, which has been widely discussed and investigated in capillary electrophoresis.

Joule Heating. An analytical Joule heating model for electrophoresis in rectangular channels, which is a good approximation to our FFIEF chip, was applied by Cifuentes and Poppe.[32]

(29) Giddings, J. C.; Dahlgren, K. *Sep. Sci.* **1971**, *6*, 345–356.
(30) Wang, Q.; Tolley, H. D.; LaFebre, D. A.; Lee, M. L. *Anal. Bioanal. Chem.* **2002**, *373*, 125–135.
(31) Hannig, K.; Heidrich, H. G. *Free-flow Electrophoresis*; GIT Verlag: Darmstadt, 1990.
(32) Cifuentes, A.; Poppe, H. *Chromatographia* **1994**, *39*, 391–404.
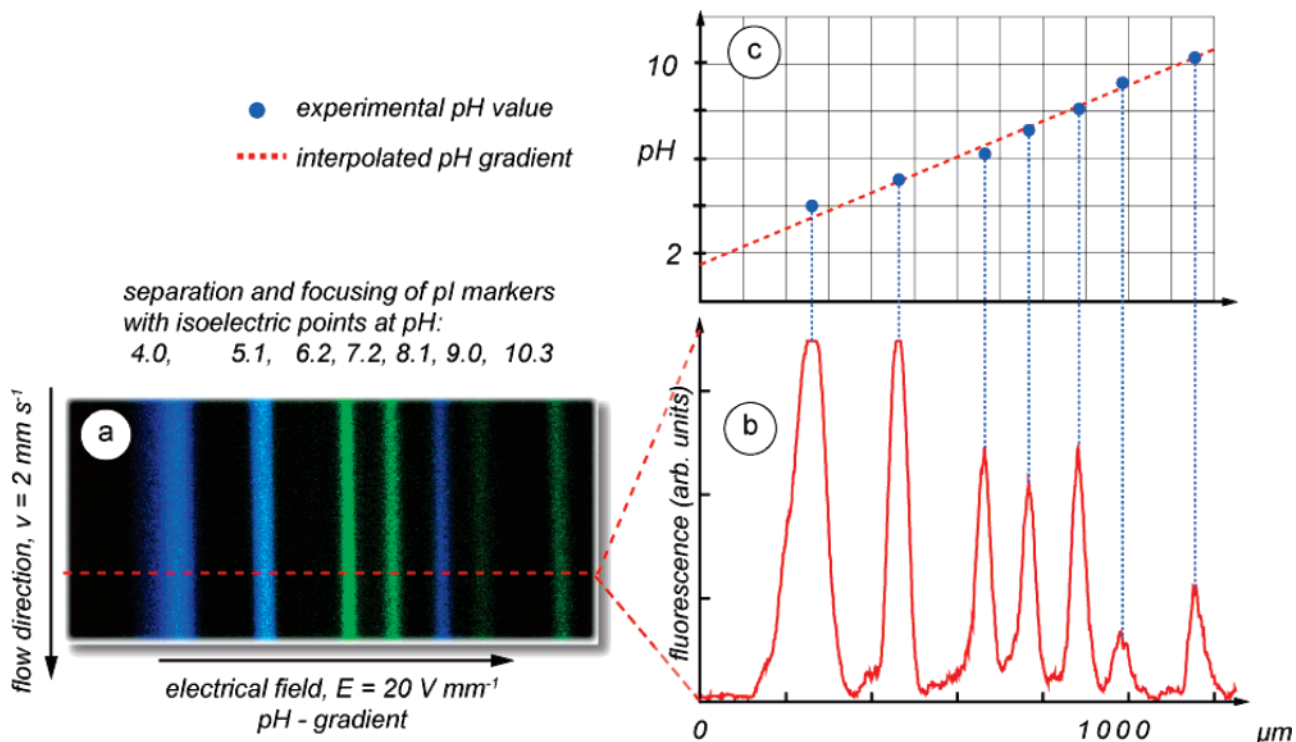
Figure 5. Analysis of the established pH gradient from various IEF markers. (a) Seven IEF markers were focused during IEF and (b) an electropherogram was generated. The experimental pH gradient was derived from the peaks positions (c). The focusing time was 2.5 s. (100 μg mL^{-1} of pI markers 4, 5.1, 6.2, and 20 μg mL^{-1} pI markers 7.2, 8.1, 9, and 10.3).

Table 1. Peak Standard Deviations for the Experimental Results Shown in Figure 5[a]

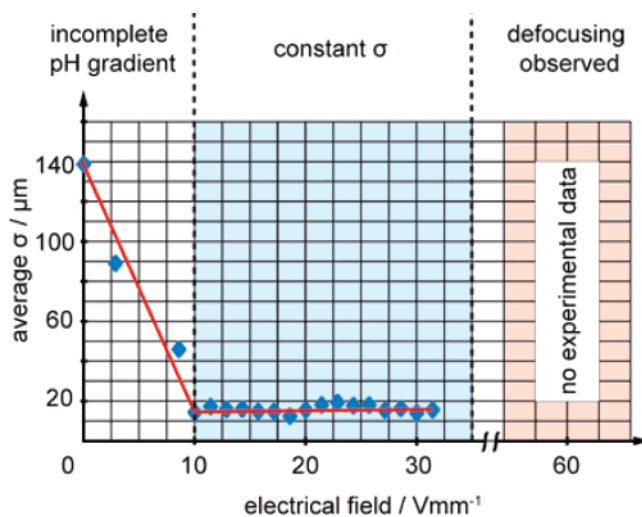|	IEF marker/pI						
	4.0	5.1	6.2	7.2	8.1	9.0	10.3
peak position x/μm	245	456	646	756	857	953	1119
peak width between inflection points w/μm	65	47	30	30	28	39	28
standard deviation σ/μm	32.5	23.5	15	15	14	19.5	14

[a] The average deviation is $\sigma_{av} = 19\ \mu$m.

Considering that the temperature gradient between the top and the bottom of the flow chamber is negligible because of the 10-μm height of the chamber, the results of Cifuentes and Poppe can be simplified to

$$T_I = T_m + W_v\left[\frac{abd}{2(a+b)k_2}\right] \tag{3}$$

where T_I is the temperature inside the separation chamber, T_m the measured temperature at the outside glass wall, a the channel height, b the channel width, d the glass wall thickness, k_2 the thermal conductivity of the wall material, and W_v the power dissipation per unit volume. W_v can be calculated from the applied voltage times the electrical current divided by the separation chamber volume. In order to obtain values for T_m, the chip outside temperature was measured using a thermocouple probe attached to the glass surface. The calculated fluid temperature and the measured electrical current are shown in Figure 7.

At electrical field strengths below 15 V mm^{-1}, a steep linear increase in current can be observed, which corresponds to the


Figure 6. Electrical field increase during FFIEF and average σ of 7 IEF markers ($\Phi_{sample} = 0.4\ \mu$L min^{-1}, $v = 2$ mm s^{-1}) determined. The plot indicates that after an initial phase where an increasing electrical field strength decreases the peak width, the peak width does not decrease further, but tends to reach a constant value.

decrease in peak width in Figure 6. We explain this rapid increase by the contribution of an increasing sorting of the ampholytes during their residence time in the device. At a flow velocity of 2 mm s^{-1}, a residence time of 5 s seems insufficient to reach a full separation of the ampholytes and thus a linear pH gradient before $E = 15$ V mm^{-1} (see also Figure 2b). Around 15 V mm^{-1}, the ampholytes become totally sorted within their residence time. Above this field strength, the further increase of current with electrical field will only represent the carrier solution conductivity plus a contribution to rectify the position of diffusing ampholytes.
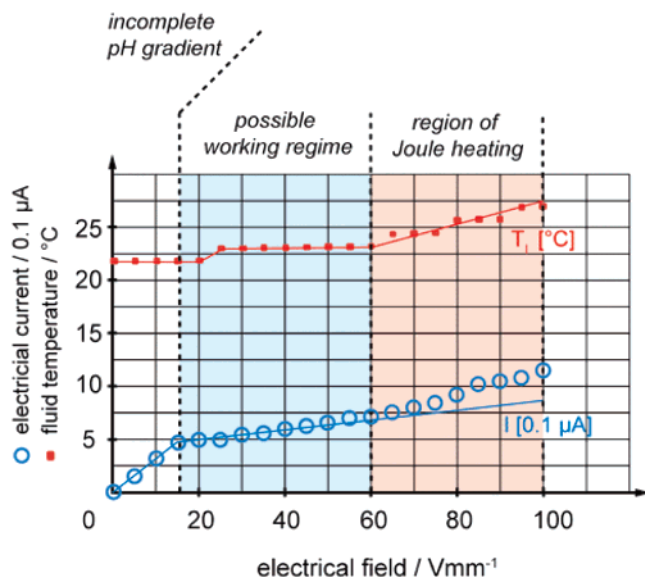
Figure 7. Three current regions distinguished as a function of electrical field. Joule heating occurs at high field strengths.
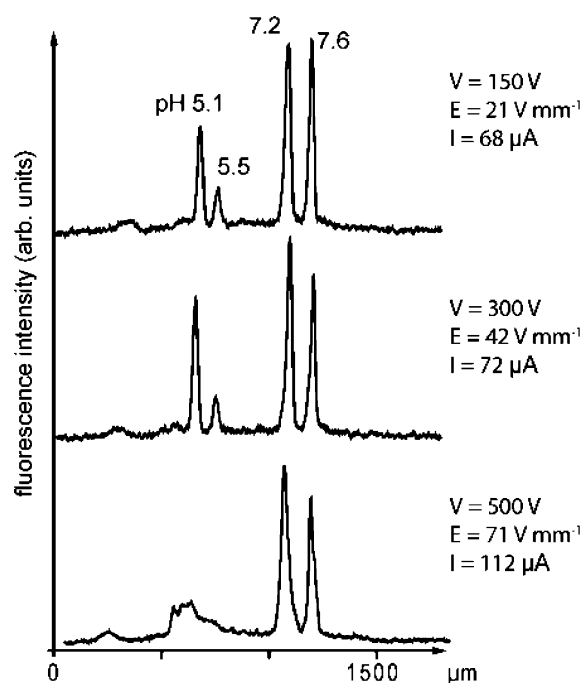
Figure 8. Three electropherograms showing the separation of 4 IEF markers. The device is capable of separating with a minimum pI difference of $\Delta(pI)_{min} = 0.4$. Best separation was achieved with 150 V (21 V/mm). Flow velocity was 2 mm s^{-1}, and the residence time $t_R = 2.5$ s (40 μg mL^{-1} IEF marker 5.1, 5.5, 7.2, and 7.6).

Between 20 and 60 V mm^{-1}, the current increases linearly, while the fluid temperature remains stable and equal to room temperature. This region corresponds to the constant peak width (σ_{av}) as shown in Figure 6. We can conclude that the device is operational up to electrical field strengths of ~60 V mm^{-1} and an electrical current of 70 μA without the influence of Joule heating. Therefore, Joule heating cannot explain the lack of peak width decrease with a increasing electrical field, which was contrary to theoretical predictions.

As shown in Figure 7, electrical fields above 60 V mm^{-1} led to Joule heating. During experiments, we observed significant band

broadening and eventually defocusing of the sample in this region (see also Figure 8). Both diffusion and fluid viscosity are highly temperature dependent. An increase in diffusion would result in band broadening, as can be seen by eq 1. Furthermore, a decreasing viscosity would increase the electroosmotic flow. Probably the combination of viscosity change and EOF destabilizes the isoelectric focusing at elevated electrical field strengths. An integrated cooling system as investigated by Albrecht and Jensen can reduce the influence of Joule heating and might allow the application of electrical fields in this region.[21]

Electroosmotic Flow. Since Joule heating seems to be negligible below 60 V mm^{-1}, it cannot explain the observed lack of peak width decrease. We assume that most likely EOF is hindering a further increase in resolution between 15 and 60 V mm^{-1}. Electroosmotic flow is directly proportional to the applied electrical field strength; thus, an attempt to improve the resolution by increasing the voltage, increases EOF as well. Although the chip surface has been PVA coated (minimizing ζ potential) and HPMC was added (increasing viscosity) to the solutions, it is uncertain to what extent EOF was suppressed. In closed channel systems, such as in our FFIEF device, electroosmotic flow near the walls will cause a hydrodynamic counterflow in the channel center.[31,33] This recirculation can obviously cause band broadening. However, it is unclear how the EOF flow profile in the case of FFIEF devices will look like, since the ζ potential and therefore the EOF are highly pH dependent. Possibly, regions of high and low EOF would exist, causing localized recirculation effects and heterogeneous band broadening, working against the focusing and limiting the device in terms of resolution. In microfluidic FFE devices, the reduced channel height is already advantageous over conventional FFE systems where channel heights of several hundred micrometers are used, since the band broadening caused by EOF is counteracted by lateral diffusion more efficiently. The influence of a parabolic flow profile can be quantified by defining an effective diffusion coefficient D_T, which represents the sum of both thermal diffusion and the convective dispersion.[34]

$$D_T = D + u^2d^2/210D \tag{4}$$

where $u^2d^2D^{-1}$ represents the dispersion caused by a pressure-driven flow with the velocity u in an indefinite wide channel with the height d. In our situation, this flow will be proportional to the EOF, and thus, u can be replaced by $u_{EOF} = \mu_{EOF}E$. Furthermore, replacing the diffusion constant D in eq 1 with the effective diffusion constant D_T from eq 4 results in

$$\sigma_{EOF} = \sqrt{\frac{1}{p}}\sqrt{\frac{D}{E} + \frac{Ed^2}{210D}\mu_{EOF}^2} \tag{5}$$

Equation 5 shows the bandwidth dependence on the electrical field when EOF is taken into account. With increasing E, the first summand does decrease σ while the second summand increases σ and compensates for this enhancement. This could explain the stabilized bandwidth observed for electrical field strengths be-

(33) Lammertink, R. G. H.; Schlautman, S.; Besselink, G. A. J.; Schasfoort, M., R. B. *Anal. Chem.* **2004**, *76*, 3018−3022.
(34) Giddings, J. C. *J. Chromatogr.* **1961**, *5*, 46−60.

tween 20 and 60 V mm^{-1}. Substituting reasonable values for D and μ_{EOF} indeed hardly any change of σ is predicted from $E = 20$ and 60 V mm^{-1}. If these considerations are correct, the further suppression of EOF ($\mu_{EOF} \rightarrow 0$) has to be the major issue to overcome current limitations in terms of resolution. Different wall coatings reducing the ζ potential or different chip materials for example could be investigated.

System Performance. A way to express the separation quality in IEF systems in terms of system properties is the minimum pI difference required for two species to be separated. It is generally expressed by

$$\Delta(pI)_{min} = (d(pH)/dx)3\bar{\sigma} \qquad (6)$$

which assumes a minimum distance between two separated peaks of 3 times σ. Another important characteristic quality parameter is the peak capacity n given by

$$n = L/4\bar{\sigma} \qquad (7)$$

where L is the total length of the pH gradient.[30]

In order to obtain experimental values for $\Delta(pI)_{min}$ and n, which are typical for analyte separations, we separated analytes with small differences in pI, namely, four fluorescent IEF markers with pI = 5.1, 5.5, 7.2, and 7.6. The experimental conditions were the same as before, except for the total width of the pH gradient, which was increased from 1.5 to 1.8 mm by adjusting the width of the outer sheath flows. The separation results are shown in Figure 8. It can be seen that all markers were clearly separated and focused. As can be seen in Figure 8, an increase in electrical field strength did not lead to a further improved separation. In contrast, defocusing was observed at field strengths higher than $E \approx 70$ V/mm, which corresponds to the theoretical considerations discussed before. Applying eqs 6 and 7, we calculated (pH 2.5−11.5 and $L = 1800\ \mu$m) a minimum pI value $\Delta(pI)_{min} = 0.23$ and a theoretical peak capacity of $n = 29$ peaks. In our previous device,[27] we were only able to reach a peak capacity of seven peaks and a minimum $\Delta(pI)_{min} = 0.7$, indicating that the present device represents an important improvement. In terms of focusing, we furthermore reached a 20-fold increase in sample concentration. Rough comparisons between the FFIEF results published by Albrecht and Jensen and our achievements indicate an 8-fold increase in peak capacity, a 4.3-fold decrease in minimum ΔpI, and a 2.6-fold reduction of the applied voltage in our device. To be fair, it must be realized, however, that Albrecht and Jensen optimized their device with respect to a higher throughput. Furthermore, comparisons should be considered with care, since many parameters have to be taken into account. In FFIEF devices, the flow rate and related to that the residence time are important parameters as well. As shown by Fonslow and Bowser using a μ-FFE system, flow rate, electric field, and migration distance must all be considered in free flow systems to optimize bandwidth and resolution.[23] Here we investigated only the influence of the electrical field on the performance with a fixed flow rate, since in our device, especially the stability of the acrylamide membranes turned out to be the limiting factor in terms of flow rates. Velocities higher than ∼4 mm s^{-1} caused breakage of the membranes often within minutes. Therefore, all experiments were carried out with a constant velocity of 2 mm s^{-1}.
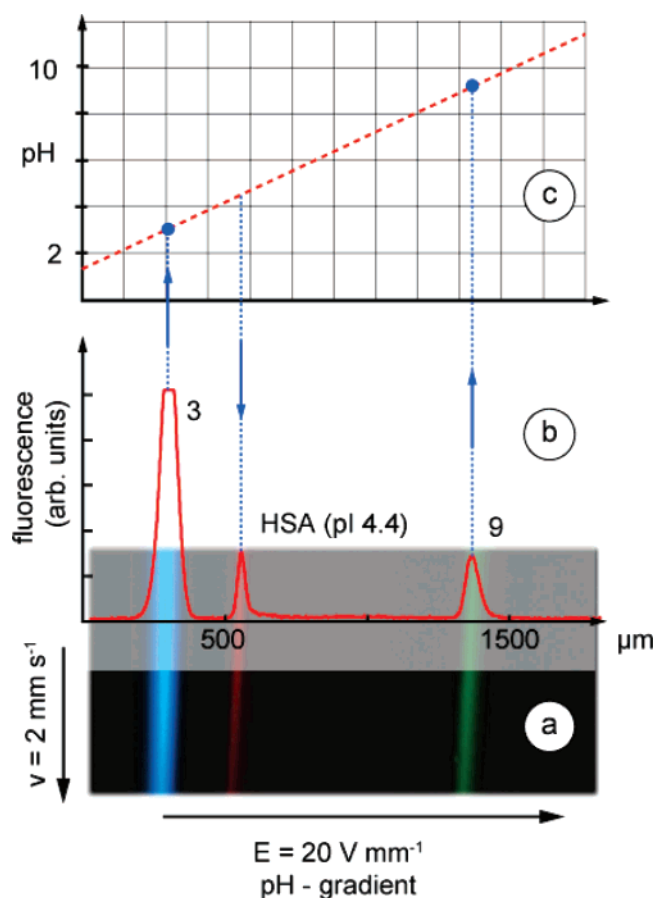
Figure 9. FFIEF of two fluorescent IEF markers (pH 3 and 9) and HSA. The focusing of the low molecular weight standards results in wider bands compared to HSA. HSA focused at the pH value 4.4. Concentrations: 330 μg mL^{-1} HSA, 80 μg mL^{-1}; IEF markers pH 3 and 9. The focusing residence time was 2.5 s.

To investigate the benefit of preseparating the ampholytes by introducing them in different inlets, an additional experiment was performed. The ampholytes prolytes1, 2, and 3 were mixed so that no stepped pH gradient was applied. Experimental results confirmed that in this case with an electrical field strength of 20 V mm^{-1} no separation was achieved within the present separation chamber length (data not shown here). Even when increasing the separation voltage and electrical field, a complete separation was not observed. This indicates the advantage of using preseparated ampholytes over common nonseparated ampholytes in microfluidic FFIEF systems, since it leads to faster separation times and therefore better resolution also observed in large-scale conventional FFIEF systems.[28]

FFIEF of Human Serum Albumin (HSA). The separation of low-MW IEF markers, as demonstrated, is a practicable model system. However, for clinical analysis, one would like to know about protein separation. Often described in the literature is a decreased separation resolution of fluorescently labeled proteins due to heterogeneous labeling. Recently, a new type of fluorescent label has been introduced, which does not alter the native charge of the protein and thus minimizes band broadening.[35] We decided to investigate these labels in our system. We chose HSA (pI ≈

(35) Craig, D. B.; Wetzl, B. K.; Duerkop, A.; Wolfbeis, O. S. *Electrophoresis* **2005**, *26*, 2208−2213.

4.8, MW 67 000) as a test protein. According to eq 2, one would expect that proteins that have a higher MW than the low-MW IEF markers (estimated MW ~500) and, therefore, a lower diffusion coefficient, which would result in better separation resolution and sharper peaks. This was indeed confirmed in an experiment using two fluorescent pI markers, pH 4 and 9, and the protein HSA. The results are shown in Figure 9. All components were fully separated (Figure 9a), and as expected, a narrower HSA peak was observed (Figure 9b). The width of the HSA peak (full width at half-maximum) is ~2 times smaller than of the IEF markers. Using the two markers as a reference, the derived pI value for HSA is 4.4 which is acceptable.

CONCLUSIONS

Microfluidic free-flow isolectric focusing was successfully demonstrated using a glass chip in which preseparated ampholytes were infused into a 350-nL separation chamber, which resulted in a more efficient generation of a linear wide range pH gradient in terms of electrical current and formation time than without preseparation. This method led to a highly improved separation resolution. We determined that the device is capable of separating analytes with a minimum difference in isoelectric point of $\Delta(pH)$ = 0.23. This results in a theoretical peak capacity of 29 peaks within 1.8 mm for a pH gradient pH 2.5−11.5. Furthermore, linearity of the pH gradient was demonstrated by the separation of seven IEF markers ranging from pH 4 to 10. All components were separated transverse to the carrier flow within 1.2 mm, and complete focusing (20-fold concentration increase) was realized in only 2.5 s. From theoretical considerations and experimental results, we concluded that band broadening caused by EOF and eventually Joule heating probably limits the separation resolution at elevated electrical field strengths. Further minimizing the EOF and integrating a cooling system might therefore lead to still higher resolution. The device was also used to focus HSA, showing that with high-MW molecules even narrower peaks can be realized. The resolution achieved was superior to all microfluidic FFIEF chips until now. This device might be applicable in clinical analysis as a preanalytical fractioning method, when only low sample volumes are available and fast separation times are necessary.